Fabrication and characterization of magnetic media deposited on top or side edges of silicon dots

Stéfan Landis, Bernard Rodmacq, Pascale Bayle-Guillemaud, Vincent Baltz, Bernard Diény

Fabrication and Characterization of Magnetic Media Deposited on Top or Side Edges of Silicon Dots

Stéfan LANDIS*, Bernard RODMACQ[1], Pascale BAYLE-GUILLEMAUD[2], Vincent BALTZ[1] and Bernard DIÉNY[1]

CEA-DRT-LETI-CEA/GRE, 17 rue des martyrs, F-38054 Grenoble Cedex 9, France
[1]*CEA/DRFMC/SPINTEC, 17 rue des martyrs, F-38054 Grenoble Cedex 9, France*
[2]*CEA/DRFMC/SP2M, 17 rue des martyrs, F-38054 Grenoble Cedex 9, France*

Arrays of lines and dots were patterned on silicon substrates by electron beam lithography and reactive ion etching. Co/Pt multilayers were sputter-deposited on these patterned substrates to realize perpendicular patterned media for ultra high-density magnetic recording. Magnetic material thus covers the top of the lines and dots, the bottom of the grooves between nanostructures, and to a lesser extent, the sidewalls. Magnetic properties were characterized by both macroscopic and magnetic force microscopy experiments. From the results obtained from high-resolution transmission electron microscopy (TEM) experiments, we propose a new approach for realizing patterned magnetic media using the side edges instead of the top of the dots.

KEYWORDS: ebeam lithography, patterned magnetic media, atomic force microscopy, magnetic force microscopy

1. Introduction

Nowadays, magnetic recording remains the most efficient and cheapest method of reversibly writing and reading massive amounts of information. In the current storage technology, which uses continuous polycrystalline thin film media, the signal-to-noise ratio (SNR) of the media is directly related to the number of grains per bit.[1)] To keep increasing the areal density in continuous layers, it is necessary to further reduce the grain size. Nevertheless, there is a physical limit to how small the grain size can be before thermal fluctuations can lead to some instability of the magnetization. This is known as the superparamagnetic limit.[2)] To go beyond densities greater than 200 Gbit/in^2, a totally different approach is required, which may use patterned media, i.e., media made of arrays of nanometer-scale individual dots in which each dot carries a bit of information.[3)] The significant advantage of such media is that the shape of the edge of each bit is not determined by the grain size as in continuous media, but is determined by the patterning process used to make the dots. Consequently, each dot can be made of a single magnetic grain (1 grain per bit instead of a few hundred grains per bit as in continuous media). The volume of the grains can therefore be much larger in patterned media so that the superparamagnetic limit is no longer a problem, and storage capacities up to several terabits per square inch may be achieved in such systems. Various techniques have been developed to prepare arrays of submicrometer magnetic dots: optical, ebeam, laser interferometry or X-ray lithography followed by the etching of the magnetic material,[4)] ion irradiation through stencil masks,[5)] patterning using a focused ion beam,[6)] and self-organization of nanoparticles.[7)] Thus far, none of these techniques seems to combine the criteria of low cost, rapid patterning of large-area (several square inches) magnetic nanostructures with the possibility of including special patterns for a servo. We have developed an original approach for preparing arrays of magnetic dots which uses prepatterned wafers on top of which a ferromagnetic material is deposited.[8)] The nanopatterning of the magnetic material directly results from its deposition on the prepatterned wafer.

In this paper, we first present the technique used to produce the patterned wafers. Then, we discuss the macroscopic and microscopic magnetic properties of (Co/Pt) multilayers deposited on the top of silicon dot arrays. We will then present structural characterizations of (Co/Pt) line and dot arrays. Finally, we propose a new approach for preparing patterned magnetic media.

2. Sample Preparation

Patterned silicon samples are prepared with electronic beam lithography on 8-inch wafers. We used a Leica VB6HR system and a negative-tone chemically amplified resist from Sumitomo Chemicals to expose line and dots arrays. After the resist development, relief lines and dots are defined on a flat sample. The best resolution achievable with this resist is 75 nm dense square dot arrays. However, we do not present in this paper this level of resolution because our main objective is to demonstrate the feasibility of our concept. Therefore, larger dots have been used to make the characterization experiments easier. A standard reactive ion etching method is used to transfer the resist patterns into silicon (Fig. 1). In this paper, we define two areas on the sample. The first is the top of the dots and the lines which are at a higher level than the rest of the sample, and the second, the groove, which is the region between the lines or dots (Fig. 1).

The last step of the preparation consists of sputter-depositing cobalt magnetic layers on a non magnetic chromium layer or Co/Pt multilayers on the entire substrate. The patterned part of the sample as well as the non patterned area is covered with magnetic material. The deposition is carried out at room temperature by dc sputtering for cobalt, chromium and platinum at a rate of about 0.1 nm/s. The surface area of the sputtering targets was about 3 inches in diameter, and the abrasion area was a 50 mm diameter ring. The cathode voltage was about 300 V for all materials with an argon working pressure in the range of 2.7×10^{-3} mbar. The distance between the target and the substrates was about 100 mm. Co layers exhibit a planar magnetization, whereas the (Co/Pt) multilayers exhibit a perpendicular magnetization.

*E-mail address: slandis@cea.fr

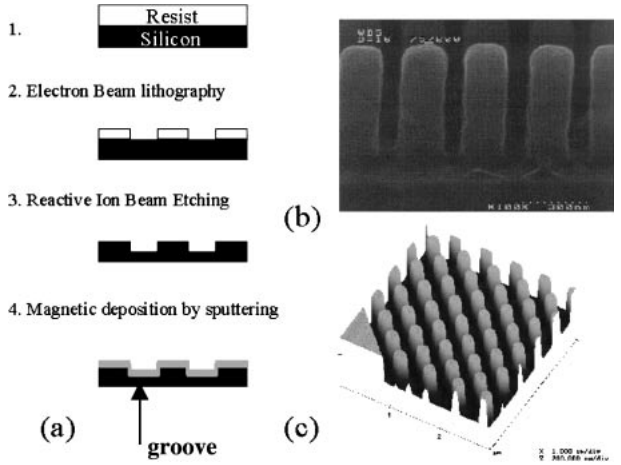

Fig. 1. (a) Lithographic preparation process, (b) scanning electron microscopy image of a 200/75/600 resist dot array, and (c) 3 μm × 3 μm AFM image of a 200/200/150 silicon dot array.

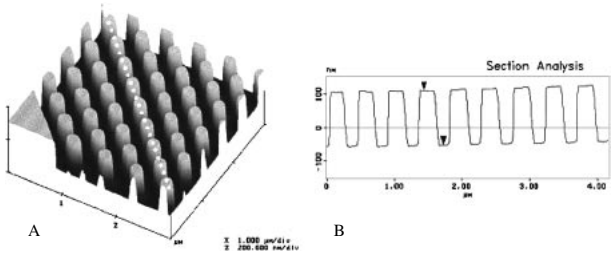

Fig. 2. (a) 3 μm × 3 μm AFM image of a 200/200/150 silicon dot array and (b) cross-sectional profile.

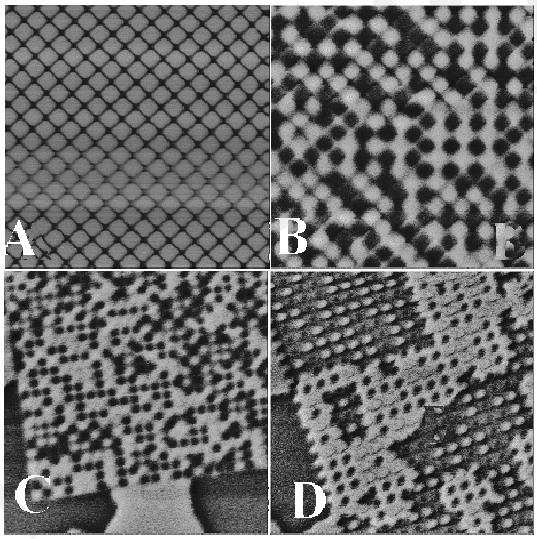

Fig. 3. 8 μm × 8 μm (a) AFM and (b) MFM images of a $Pt_{1.8\,nm}$ $(Co_{0.6\,nm}/Pt_{1.8\,nm})_4$ multilayer deposited on a 400/100/47 dot array. 8 μm × 8 μm MFM images of a $Pt_{1.8\,nm}$ $(Co_{0.6\,nm}/Pt_{1.8\,nm})_4$ multilayer deposited on (c) 200/100/47 and (d) 200/200/47 dot arrays.

Macroscopic magnetic experiments on both continuous and patterned samples were carried out using the polar Kerr effect and SQUID measurements. Atomic force microscopy (AFM) and magnetic force microscopy (MFM) were performed with a Digital Instrument Nanoscope IIIa, in tapping mode.[9] For the MFM measurements, the image was obtained with a two-step lift mode[10] process, the first scan being used to determine the topography and the second one passing at a fixed height above the known surface while recording the magnetic response of the tip with a phase detection system. During imaging, the tip is magnetized in the direction perpendicular to the sample surface. MFM tips were prepared in our laboratory by sputter-depositing a $Co_{80}Cr_{20}$ alloy on silicon tips. Transmission electron microscopy (TEM) experiments were performed with a JEOL 4000EX microscope operating at 400 kV with a spatial resolution of 0.16 nm.

The silicon lines and dots used in this present study are identified in the rest of this paper by ($L/d/h$), where L is the size of the lines or square dots, d their edge to edge spacing and h their height.

3. Magnetic Properties of Multilayers deposited on the Top of Patterned Substrates

Continuous (Co/Pt) multilayers exhibit a magnetic anisotropy perpendicular to the film plane. They have been extensively studied,[11] and their magnetic properties can be tuned by adjusting the layer thickness of cobalt and/or platinum or by adjusting the number of multilayers. In this section, we present the magnetic properties of $Pt_{1.8\,nm}$ $(Co_{0.6\,nm}/Pt_{1.8\,nm})_4$ multilayers on pre-patterned substrates. Domain structures and the mechanism of the magnetization reversal of this multilayer on flat wafers have already been published.[12]

Figure 2(a) is a three dimensional AFM image of 200/200/47 silicon dots, and Fig. 2(b) is a cross-sectional profile along the dotted white line on Fig. 2(a). These images show the good regularity and quality of the array. In Fig. 2(a), the dots appear cylindrical rather than square. However, this is an artifact of the AFM measurement, as there is a convolution between the corners of the dots and the AFM tip. Therefore, dots appear much rounder than they actually are.

Figure 3 shows the AFM and MFM images of several dot arrays covered with a $Pt_{1.8\,nm}$ $(Co_{0.6\,nm}/Pt_{1.8\,nm})_4$ multilayer. Figure 3(a) is an 8 μm × 8 μm AFM image of the 400/100/47 arrays, and Fig. 3(b) is the corresponding magnetic image in the as-deposited state (i.e, without any magnetic treatment). A uniform white or dark contrast is seen on each dot, which indicates that the dots are single domains. All sizes investigated (400, 300 and 200 nm) led to the same observation. The 100 nm spacing between dots does not allow the tip to explore the magnetic configuration at the bottom of the grooves.

Figure 3(c) is a MFM image of the 200/100/47 array in the as-deposited state. We can see again that each dot corresponds to a single magnetic domain. Furthermore, we can also see that the size of the magnetic domains (a few microns) in the non patterned part of the sample (bottom of image 3c) is much larger than the dot size and corresponds to that observed in macroscopic samples.[12]

Figure 3(d) is a MFM image of the 200/200/47 array in the as-deposited state. In this case, the spacing between dots is sufficiently large (200 nm) to allow the tip to explore the magnetic configuration at the bottom of the grooves. The continuous magnetic medium within the grooves has a domain size of about 3–4 μm, comparable to that observed

on the flat part of the wafer (bottom left of the image). In this figure, it also appears that the magnetization of the dots can be up or down, whatever the magnetization direction in the grooves. This shows that there is no significant direct exchange coupling between the magnetic material at the top of the dots and in the grooves via a magnetic deposit, which may exist on the sidewalls of the dots. This confirms that if any magnetic deposit is present on the walls, its thickness must be much smaller than the nominal one.

4. Structural Characterizations

To correlate magnetic configurations in dot arrays and the structural properties of the deposited multilayers, we performed AFM and high-resolution TEM experiments on magnetic line arrays prepared in the same way as the dot arrays and under the same conditions. No dot arrays have been characterized by cross-sectional TEM experiments, because this technique requires a thinning down of samples. Indeed, because with dot arrays the probability of finishing the thinning down in a groove was high, we decided carried out these observations on line arrays. Of course, results obtained on lines are completely transposable to dots, because dimensions and deposition conditions in both systems are similar.

Figure 4 shows AFM images of 200/200/36 silicon line arrays before (Fig. 4(a)) and after (Fig. 4(b)) the deposition of a $Pt_{24\,nm}$ $(Co_{0.6\,nm}/Pt_{1.8\,nm})_4$ multilayer. The cobalt was deposited at a normal incidence angle, and the platinum, at an oblique incidence angle of 36° from the normal to the film plane. The AFM images show that the geometry is not modified and that the lines are still well defined even if the total thickness of the deposit is almost as large (34 nm) as the height of the lines (36 nm). Cross-sectional profiles (Fig. 4(c)) reveal that the height of the lines before and after the deposition of the multilayer is the same, which implies that the same amount of material is deposited on the top of the lines and at the bottom of the grooves. Moreover, the width of the lines after deposition (255 nm) is larger than its initial width (216 nm); this increase compensates for the reduction in the spacing between neighboring lines. This larger width is due to the amount of platinum obliquely deposited on the sidewall. It must be noticed that both AFM images were obtained with the same tip under the same conditions. Therefore, the modification of the profiles cannot be attributed to the tip's convolution with lines.

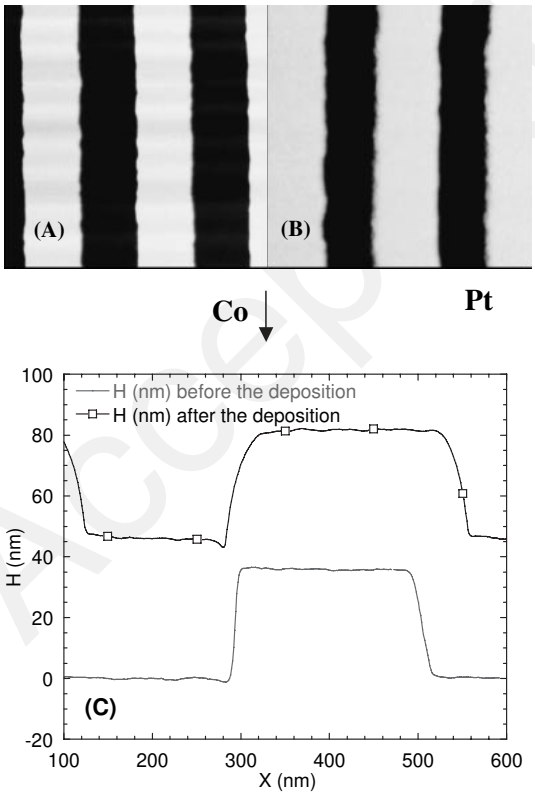

Fig. 4. 1 µm × 1 µm AFM images of 200/200/36 line arrays (a) before deposition and (b) after deposition of a $Pt_{24\,nm}$ $(Co_{0.6\,nm}/Pt_{1.8\,nm})_4$ multilayer. (c) Cross-sectional profiles of AFM images (a) and (b). Cobalt and platinum incidence fluxes are represented on the cross-sectional profile curves.

Because it was not possible with AFM to determine precisely the amount of material deposited on the sidewalls of the lines and its chemical composition, TEM cross-sectional images were recorded. Figure 5 is a TEM image of the $Pt_{1.8\,nm}$ $(Co_{0.6\,nm}/Pt_{1.8\,nm})_4$ multilayer (i.e, the same as in Figure 4 without the 24 nm Pt buffer) deposited on the 150/100/36 line array. Normal and oblique incidences were also used for cobalt and platinum, respectively. The multilayer is well defined on the top and at the bottom of the groove, and all Co and Pt layers can easily be identified. The continuous line with a bright contrast between the silicon and the multilayer comes from the native silicon dioxide (∼2 nm). This image also shows that the multilayered structure is strongly perturbed on the sidewalls of the line. Indeed, on the left sidewall, which did not face the platinum flux, one can only observe small aggregates identified as cobalt oxide grains,[13] whereas on the right sidewall the deposit seems to follow the topography of the sample. Nevertheless, the multilayer is not continuous on this sidewall. We performed a chemical analysis of this deposit, and essentially only platinum was found with a grain size comparable to that in the multilayer on the top of the line.[13] This explains why there is no direct magnetic exchange coupling between the top of the lines and the bottom of the grooves. Finally, in the groove at the bottom of the left sidewall, the thickness of the multilayer decreases progressively due to the shadowing effect of the platinum flux. This is also observed on the AFM image (Fig. 4(c)) on the curve representing the topography after the deposition, although the AFM image has a smaller spatial resolution than the TEM image. Figure 5 reveals that the sputtering process is quite directional and that, depending on the deposition conditions and the dimensions of the arrays, it is possible to control the chemical composition of the material deposited at the bottom of the grooves and the top of the lines and the sidewalls.

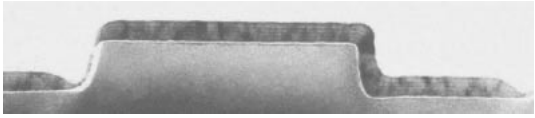

Fig. 5. TEM image (457 nm × 370 nm) of a $Pt_{1.8\,nm}$ $(Co_{0.6\,nm}/Pt_{1.8\,nm})_4$ multilayer deposited on a 150/100/36 line array.

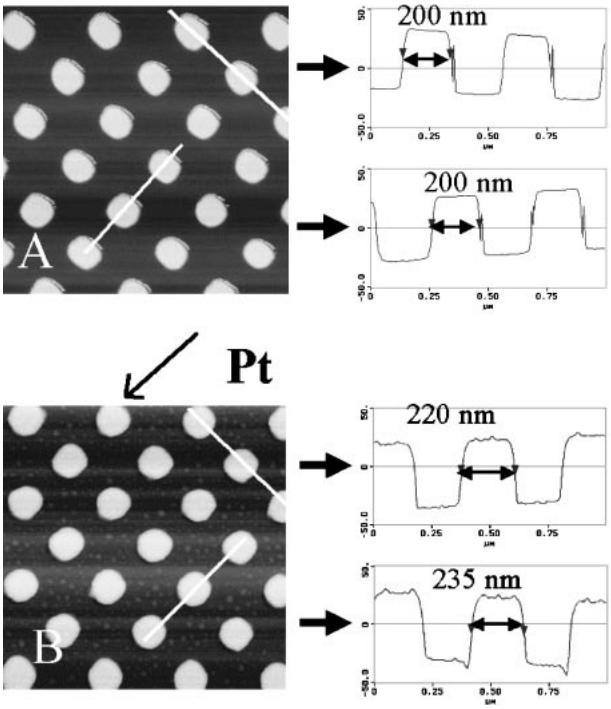

Fig. 6. $2\,\mu m \times 2\,\mu m$ AFM images of 200/200/47 dot arrays (a) before deposition and (b) after deposition of a $Pt_{20\,nm}$ $(Co_{0.6\,nm}/Pt_{1.8\,nm})_4$ multilayer, and associated cross-sectional profiles. The platinum incidence flux is also represented.

As the preparation of the dot arrays is similar to that of the line arrays, most results obtained from TEM experiments on lines can be transposed to dots. Therefore, we performed AFM experiments before and after the deposition to quantify, although with a lower resolution than with TEM, the changes in topography. Figure 6 shows two AFM images with cross-sectional profiles for two perpendicular directions (parallel or perpendicular to the platinum flux), obtained with the same tip and under the same conditions on a 200/200/47 dot array covered with a $Pt_{20\,nm}$ $(Co_{0.6\,nm}/Pt_{1.8\,nm})_4$ multilayer. The direction of the platinum flux is represented in Fig. 6(b). Before the deposition (Fig. 6(a)), the size of the dots and profiles are similar in both directions, whereas after the deposition (Fig. 6(b), both the width and profile are different along and perpendicular to the direction of the platinum flux. For the sidewalls parallel to the platinum incidence, the profile is similar to that observed before the deposition, although the width is 20 nm larger. Electron microscopy experiments on samples prepared with both Pt and Co normal incidences have shown that the amount of material deposited on each sidewall corresponded to about 24% of the nominal thickness. One thus expects an increase in dot width of about 14 nm (the total thickness deposited on the top of the dots is 30 nm), in agreement with the experimental result (20 nm). For sidewalls perpendicular to the platinum flux, the width is also larger and we can observe a small dip at the bottom of the sidewall opposite to the platinum flux (the black circle on the profile curve). This topographic signal is actually the same as that observed in the groove of the line array in the TEM image (Fig. 5). Therefore, we can conclude that only a few cobalt grains have been deposited on this sidewall, whereas an almost pure platinum layer covers the other sidewall facing the platinum flux. The total width of the dot in that direction should thus increase by about 28 nm (the total Pt thickness of 27 nm deposited on the top of the dot and the equivalent 0.6 nm Co layer), in agreement with the experimental value (35 nm).

From the magnetic point of view, the side-walls parallel to the Pt flux are thus covered with a non-magnetic $Pt_{4.8\,nm}/(Co_{0.14\,nm}/Pt_{0.43\,nm})_4$ multilayer, whereas the sidewall facing the Pt flux is covered with a 27 nm Pt layer and the other sidewall is covered with a very thin and probably superparamagnetic Co layer (four sequentially deposited Co layers with a thickness of 0.14 nm) for. This explains why there is no magnetic direct exchange coupling between the top of the dots and the grooves.

5. Magnetic Properties of Multilayers Deposited onto the Sidewalls of Patterned Substrates

Compared to magnetic dot arrays with a magnetization parallel to the film plane, it is often easier with perpendicular magnetization systems to obtain single domain dots or particles. Nevertheless, the stray fields generated by the dots in perpendicular magnetized dots are lower, because very thin layers or multilayers are required to obtain a perpendicular magnetization, and therefore, the total amount of magnetic material (i.e, the total magnetization) in such films is lower than that in films with an in-plane magnetization.

To compensate for this reduction of the stray field, we propose a new approach which takes advantage of shadowing effects in patterned samples[14] using on oblique incidence for the magnetic deposit. This technique has already been used for continuous media;[15,16] however, it has never been used to prepare dot arrays for magnetic recording. By depositing of a thin magnetic layer with a planar magnetization onto the sidewall of a dot, the film's plane becomes perpendicular to the sample surface. Therefore, if the material presents an in-plane magnetic easy axis, the magnetization becomes either parallel (dot A in Fig. 7) or perpendicular (dot B in Fig. 7) to the sample surface. In the second case, the system is identical to a multilayer with perpendicular anisotropy deposited on the top of the dots.

We applied this approach using cobalt and chromium depositions, both with opposite oblique incidences. In this configuration, pure cobalt and chromium layers are deposited on opposite sidewalls, whereas a CoCr alloy covers the top of the dot (Fig. 8). This CoCr alloy can be made non-magnetic[17] by adjusting the Co and Cr deposition rates.

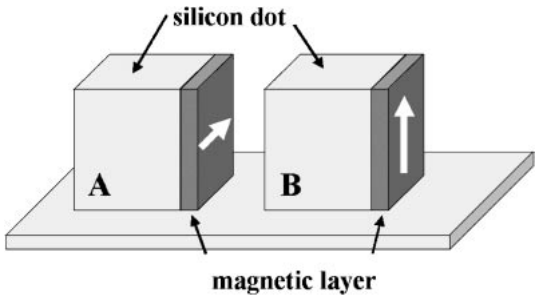

Fig. 7. Schematic representation of the magnetic deposition on dot sidewalls using oblique incidence.

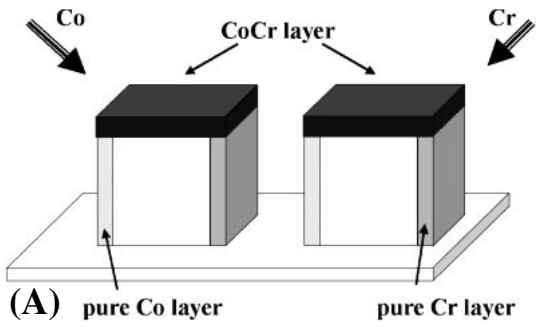

Fig. 8. Schematic representation of the deposition of cobalt and chromium on dot sidewall using oblique incidence.

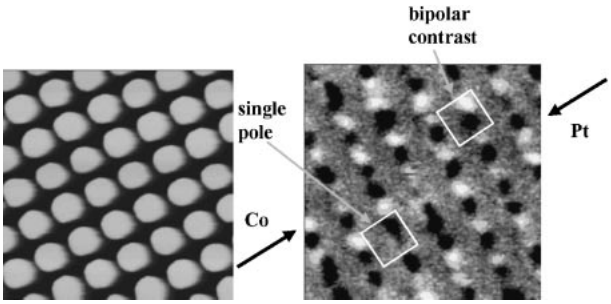

Fig. 9. $2\,\mu m \times 2\,\mu m$ AFM image (left) and MFM image (right) of (Co, Cr) deposition on the sidewalls of a 200/100/150 dot array. The Co and Pt incidences are represented on the MFM image. The white boxes represent limits of the corresponding dots.

We carried out two types of deposition on the silicon dot arrays. First, cobalt and chromium were directly deposited onto silicon dots. Then, to favor an easy magnetic axis perpendicular to the sample surface, we performed the deposition of Co and Cr on dots already covered with a (Co/Pt) multilayer with perpendicular magnetic anisotropy. The idea was to use the stray field generated by the (Co/Pt) multilayer to induce a coupling with the cobalt layer deposited on the sidewall.

Figure 9 shows AFM and MFM images in the as-deposited state for the oblique deposition of cobalt and chromium on a 200/100/130 dot array (without a Co/Pt multilayer). The Co and $Co_{60}Cr_{40}$ alloy thicknesses are about 25 nm and 50 nm, respectively. We can see that only one out of the four sidewalls contributes to the MFM signal. Therefore, oblique incidence deposition and shadowing effects can be used to create vertical magnetic nanostructures. Concerning the magnetic configurations, most of the contrast on each dot is of the dipolar type, which implies that the magnetic configuration in the Co layer is a single domain with an in-plane magnetization parallel to the surface of the sample. Only a few dots present a single magnetic pole characteristic of a single domain configuration. In this case, the magnetization is still in-plane but perpendicular to the sample surface.

Figure 10 presents AFM and MFM images of obliquely deposited cobalt and chromium on 400/100/130 and 200/100/150 dot arrays already covered with a $Pt_{1.8\,nm}/(Co_{0.6\,nm}/Pt_{1.8\,nm})_4$ multilayer. Both the as-deposited and remnant states (i.e, after having saturated the sample in a positive external magnetic field) were characterized. No difference

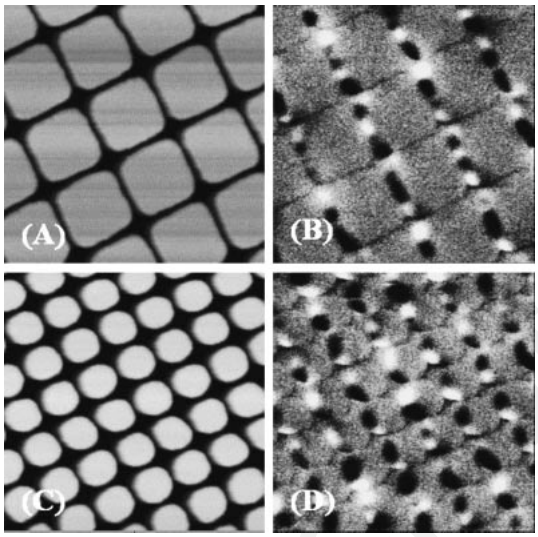

Fig. 10. $2\,\mu m \times 2\,\mu m$ AFM (a, c) and MFM images (b, d) of a (Co, Cr) deposition onto a $Pt_{1.8\,nm}/(Co_{0.6\,nm}/Pt_{1.8\,nm})_4$ multilayer on 400/100/130 (a, b) and 200/100/150 (c, d) dot arrays. The MFM images were recorded in the remnant state.

was observed, despite the fact that the magnetic configuration of the (Co/Pt) multilayer was uniform in the remnant state (the same magnetization direction for all dots), which should in principle simplify the interpretation of the MFM images.

As in the previous case, the magnetic signal is only observed at one sidewall. For, 400-nm-wide dots (Figs. 10(b)), the magnetic configuration is complicated and the magnetization is not preferentially oriented perpendicular to the sample surface. For 200-nm-wide dots (Fig. 10(d)), we find again dipolar contrast and slightly more single magnetic poles than in Fig. 9. Therefore, the (Co/Pt) multilayer leads to a slight increase in the number of single domain dots with the desired magnetization orientation. Further experiments must be carried out to create an easy magnetic axis perpendicular to the sample surface, as for example with thermal treatments under magnetic fields or using different shaped dots. Anti ferromagnetic and ferromagnetic materials deposited on dot arrays[18] may also be used to enhance the coercive field of the magnetic layer and the magnetic anisotropy along the field cooling direction. Therefore, because in such a system the magnetization does not increase, the stability of magnetic recording media will be improved and the dipolar interaction between neighboring dots will not be sufficiently strong to switch the magnetization.

This approach offers a number of advantages compared to the previous ones in which the top of the dots was the useful part for information storage. In this case, the two opposite sidewalls can be covered with magnetic material, allowing the doubling of the storage density for the same dot geometry. Such media could be obtained by first depositing simultaneously Co at an oblique incidence and Cr at a normal incidence to cover one side-wall with pure cobalt, and then turning the array by 180° in its plane to deposit Co on the opposite side-wall, the top of the dots being covered with a non-magnetic CoCr alloy. Moreover, it is conceivable to realize dot arrays with a soft layer below the magnetic

dots to enhance the perpendicular head field component from a recording head. Indeed, this requirement can be achieved using a substrate with a magnetic soft layer deposited first and then coated with another layer such as silicon or silicon dioxide. Then the standard patterning process could be used on such substrate, with the etching step stopped at the soft magnetic layer.

6. Conclusion

We showed in this paper that pre-patterned substrates could be used to realize patterned magnetic media. (Co/Pt) multilayers were deposited on line and dot arrays. Single magnetic domains with a magnetization perpendicular to the film plane were obtained. No direct exchange coupling was observed between the top of the dots and the grooves. Moreover, structural characterizations show that the topography of patterned samples was only slightly modified after deposition. TEM images reveal that the structures of the multilayers in the grooves and on the top of the dots or lines are similar and that no magnetic layer is deposited on the sidewalls, which is in agreement with the magnetic results. These experiments also show that, using oblique incidences, it is possible to control the chemical composition of layers on sidewalls, top and grooves of patterned samples. From these observations we propose a new approach for realizing magnetic patterned media by depositing a magnetic layer on the sidewalls of dots. Using cobalt and chromium layers obliquely deposited on silicon dots, MFM images reveal that the magnetic signal only comes from the sidewalls, which is a promising result for this approach.

1) R. L. White: J. Magn. & Magn. Mater. **209** (2000) 1.
2) P. L. Lu and S. H. Charap: IEEE Trans. Magn. **31** (1995) 2767.
3) S. Y. Chou, M. Wei, P. R. Krauss and P. B. Fischer: J. Vac. Sci. & Technol. B **15** (1997) 2897.
4) O. Fruchart, J. P. Nozieres, B. Kevorkian, J. C. Toussaint, D. Givord, F. Rousseaux, D. Decanini and F. Carcenac: Phys. Rev. B **57** (1998) 2596.
5) B. Terris *et al.*: Appl. Phys. Lett. **75** (1999) 403.
6) J. Lohau and A. Moser: Appl. Phys. Lett. **78** (2001) 990.
7) S. Sun *et al.*: Science **287** (2000) 1989.
8) S. Landis, B. Rodmacq, B. Dieny, B. Dal'Zotto, S. Tedesco and M. Heitzmann: Appl. Phys. Lett. **75** (1999) 2473.
9) Tapping mode is a registered trademark of Digital Instrument.
10) Lift mode is a registered trademark of Digital Instrument.
11) Z. G. Li, P. F. Garcia and Y. Cheng: J. Appl. Phys. **73** (1993) 2433.
12) S. Landis, B. Rodmacq and B. Dieny: Phys. Rev. B **62** (2000) 12271.
13) S. Landis, P. Bayle and B. Rodmacq and B. Dieny: to be published in J. Appl. Phys.
14) B. Rodmacq, S. Landis and B. Dieny: Patent application, N° E.N. 0108869 (2001).
15) K. Tanahashi, Y. Hosoe and M. Futamoto: J. Magn. & Magn. Mater. **153** (1996) 265.
16) H. Aitlamine, L. Abelman and I. B. Puchalska: J. Magn. & Magn. Mater. **71** (1992) 353.
17) T. B. Massalski: *Binary Alloy Phase Diagrams* (ASM International, Materials Park, Ohio, 1996).
18) V. Baltz, J. Sort, S. Landis, B. Rodmacq and B. Diény: submitted to Appl. Phys. Lett.